



Contents lists available at ScienceDirect

## Computer Communications

journal homepage: [www.elsevier.com/locate/comcom](http://www.elsevier.com/locate/comcom)

## A few bits are enough: Energy efficient device-free localization

Pan Wu<sup>a</sup>, Xiaobing Wu<sup>a,\*</sup>, Guihai Chen<sup>a,b</sup>, Mengfan Shan<sup>a</sup>, Xiaojun Zhu<sup>a,c</sup><sup>a</sup>State Key Laboratory for Novel Software Technology, Nanjing University, Nanjing, Jiangsu 210023, China<sup>b</sup>Shanghai Key Laboratory of Scalable Computing and Systems, Shanghai Jiao Tong University, Shanghai 200240, China<sup>c</sup>College of Computer Science and Technology, Nanjing University of Aeronautics and Astronautics, Nanjing, Jiangsu 211106, China

## ARTICLE INFO

## Article history:

Received 29 May 2014

Revised 28 October 2015

Accepted 22 January 2016

Available online xxx

## Keywords:

Device free localization

KL-divergence

Kalman filter

## ABSTRACT

A Device Free Localization (DFL) system can locate and track people wearing no wireless devices, due to the fact that a person standing at different locations attenuates wireless links differently. Since the DFL system usually consists of battery-powered sensors, energy efficiency is a critical issue. However, existing works mainly focus on improving localization accuracy by designing various metrics to characterize wireless link attenuation, and none of them considers energy efficiency, specifically. We present EE-Loc, an energy efficient localization system, for locating and tracking people with higher energy efficiency and comparable localization accuracy compared to the state-of-the-art DFL systems. EE-Loc has two main energy efficient components. First, EE-Loc has a radio tomographic imaging (RTI) component that uses only *one bit* information to describe link attenuation. The one bit information is derived from the Kullback–Leibler divergence (KL-divergence) of Received Signal Strength (RSS), and we prove that RTI with this one bit information is sufficient for localization. Second, EE-Loc has a tracking component that deactivates many unnecessary links through predicting the person's location with Kalman filter to reduce energy consumption. We build a test-bed of EE-Loc using 16 sensors. The experimental results indicate that EE-Loc improves energy efficiency by 27.05% compared to Spin\* for locating a person, and reduces link measurements by 41.91% for tracking a person, without compromising the localization accuracy.

© 2016 Published by Elsevier B.V.

## 1. Introduction

Device free localization (DFL) with wireless sensor networks can be applied to many scenarios including future healthcare, smart building and security applications [1,2]. DFL technologies are distinct from traditional localization methods in that they do not assume the targets wear any electronic devices such as RFID tags. This 'noninvasive' property is especially useful for surveillance systems where the intruders might be device-less. Typically, DFL technologies utilize the attenuation of wireless links caused by human presence to locate people. The attenuation of a wireless link can be characterized by the Received Signal Strength (RSS) change. DFL with wireless sensors can be implemented conveniently because RSS can be easily measured from most sensor platforms.

Existing DFL systems [2–5] mainly target at high localization accuracy. Therefore, various RSS dynamic measures have been proposed to characterize the attenuation caused by human presence, such as difference of mean RSS readings [2], variance of RSS read-

ings [3] and the Kullback–Leibler divergence (KL-divergence) of two RSS reading distributions [6]. A better measure for RSS dynamic values leads to a better localization accuracy. However, to calculate the proposed RSS dynamic values, raw RSS readings from all links should be sent to the base station. Higher traffic consumes the energy of every sensor much more quickly, resulting in a shorter network lifetime. Unfortunately, this important issue has not been addressed in existing DFL systems.

We aim at improving the energy efficiency of DFL systems without sacrificing the localization accuracy. This is achieved through the following observations. First, RSS readings in most platforms (such as the TelosB platform [7]) are represented by an 8-bit integer. We can finish a round of RSS collection much more quickly and put the network in sleep mode if the RSS dynamic values can be calculated locally in sensors and represented by fewer bits. Second, not all wireless links are necessary in tracking a moving person since a person can only attenuate a few links of the system. Accordingly, many sensors can turn off their radio modules to save energy if we can predict the location of the person.

We design EE-Loc, an energy efficient DFL system based on the above observations. EE-Loc contains two energy efficient mechanisms: radio tomographic imaging with binarized KL-divergence (referred to as KLDB in this work) and reducing unnecessary link

\* Corresponding author. Tel.: +86 25 8968 6659.

E-mail addresses: [panwunju@gmail.com](mailto:panwunju@gmail.com) (P. Wu), [wuxb@nju.edu.cn](mailto:wuxb@nju.edu.cn), [barry-wuh@gmail.com](mailto:barry-wuh@gmail.com) (X. Wu), [gchen@nju.edu.cn](mailto:gchen@nju.edu.cn) (G. Chen), [nju.mfshan@gmail.com](mailto:nju.mfshan@gmail.com) (M. Shan), [xzhu@nuaa.edu.cn](mailto:xzhu@nuaa.edu.cn) (X. Zhu).

measurements with Kalman filter when tracking a person. In radio tomographic imaging with KLDB, we derive one bit KLDB from KL-divergence of a wireless link to represent the RSS dynamic of the link and implement the RSS dynamic calculation locally in the wireless sensor network. Compared with other DFL systems, sensors in EE-Loc only report one bit KLDB, instead of 8-bit raw RSS reading, for each wireless link. This reduces the payload size of packets in EE-Loc. With the decrease of the payload size, the time consumption of data collection module in EE-Loc is only 65.11ms, which is 27.05% shorter than that of Spin\*, an improved version of Spin [2]. Our indoor and outdoor experiments demonstrate that EE-Loc does not compromise its localization accuracy compared to the existing work although it transmits less bits. For tracking a person, EE-Loc uses Kalman filter to predict next possible region of the person, and turns off receivers of unrelated links to save energy. Our experiments show that this mechanism reduces the link measurements by about 41.91% in each round of data collection.

The rest of the paper is organized as follows. Section 2 presents the related works. Section 3 introduces the background of device free localization. We give an overview of EE-Loc in Section 4, and present our design of EE-Loc in Section 5. Section 6 presents the experimental results and Section 7 concludes the paper.

## 2. Related works

Localization in wireless sensor networks has long been an important research issue [2,3,5,6,8–12]. Since [3,8] introduce the concept of RF-based device-free localization, several RF-based DFL systems have been implemented with wireless sensor networks. In this section we examine existing research related to RF-based DFL systems.

Fingerprinting is widely used tool in indoor localization. In [1,13], fingerprinting has been successfully applied for locating people in DFL systems. A passive radio map is constructed offline. With the map, distance in signal strength space is used as the RSS dynamic value to locate people. Moreover, Kalman filter is used to improve the tracking performance [13]. A more advanced tool, namely Support Vector Regression (SVR), is utilized to build a real-time and scalable DFL system [12]. The surveillance field is divided into many triangular areas. SVR is then used to locate people in each triangular area. Both fingerprint-based method and SVR-based method are required to collect a large amount of labeled training data, which is a time consuming step for DFL systems. One way to get rid of the burden of collecting labeled training data is to derive link model from training data. In [3,14], Zhang et al. propose a link-centric coverage model and design several geometric algorithms to locate and track targets. A more accurate fade-level skew-Laplace signal strength model is introduced in [15]. Based on experimental data, the new link model is characterized by the skew-Laplace distribution, which takes the fade level into consideration.

Radio Tomographic Imaging (RTI) [2] images the attenuation caused by human presence in the surveillance field. Wilson and Patwari propose a linear model for using RSS difference to obtain images of moving targets in a RTI system. In their later work [9], the variance of RSS readings is used as a new RSS dynamic measure to detect human motion. Considering the inaccuracy of RSS readings, Zhao and Patwari [16] propose a subspecies decomposition method to eliminate noise in RSS readings. They show that using RSS readings projected onto the extrinsic subspace has a better accuracy in location and tracking. Recently, Zhao et al. [6] adopt the kernel distance as an RSS dynamic measure to locate and track both stationary and moving people without calibration.

Besides RTI, there exist other methods to locate and track people in RF-based DFL systems. Chen et al. [4] utilize a sequential Monte Carlo (SMC) method for tracking targets and design an online EM algorithm to find location for sensors. In this

way, an RSS-based DFL system can be deployed rapidly. Zheng and Men [17] model the RSS distribution of a wireless link as a mixture of Gaussians. They propose an online learning algorithm to update the model and detect the affected links to locate a person. In [5,18], Xu et al. design a device-free localization method based on probabilistic classification and extend the DFL techniques to count and locate multiple targets in the surveillance field. In [19,20], compressive sensing is introduced to recover the sparse 'signal' in the DFL problem. Considering the high computation cost of compressive sensing based recovery, Yang et al. [19] propose a lightweight compressed maximum matching select algorithm. The notion of the correlated link is introduced to reduce the number of necessary RSS measurements.

Different from existing works that focus on improving the accuracy of DFL systems, we exploit some merits of KL-divergence and prediction of human presence to improve the energy efficiency of DFL systems. To achieve energy efficiency, we propose two energy saving mechanisms in our DFL system EE-Loc. The first mechanism is to save energy by efficiently reducing packet payload size. We notice that in some RTI systems [2,6] RSS readings of sensors are first transmitted to a base station, and are then processed into RSS dynamics on the PC. The RSS dynamics are later fed as input to the RTI algorithm. In our method, computation of RSS dynamics can be done locally in the wireless sensor network and RSS dynamics, other than raw RSS readings, are transmitted to the base station. We provide a new metric called KLDB derived from KL-divergence to represent the RSS dynamic of a wireless link with only one bit. Our method reduces the payload size of each packet compared with other DFL systems. Meanwhile, we show that the new metric can be efficiently implemented in commercial off-the-shelf sensors. The second mechanism is to save energy by decreasing the number of link measurements when tracking a person. In EE-Loc, we adopt Kalman filter to predict the possible region of the person and then turn off receivers of unrelated links to save energy, which is different from predicting possible regions with maximum speed of the person [19].

## 3. Background

DFL systems are characterized by link model and RSS dynamic measures adopted in these systems. In this section, we first revisit a classical link model in RTI, and then we describe a RSS dynamic measure called KL-divergence.

### 3.1. Link model

Human presence attenuates wireless signals of sensors deployed in the surveillance field. Based on the fact, RTI 'images' the attenuation caused by human presence. In RTI, an elliptical model [2,14] characterizes the relation between the attenuation of a wireless link and position of a person near the link. With RSS dynamic measures of many wireless links and the elliptical model, we can locate the person in the surveillance field. Next, we formally introduce the linear formulation of RTI.

A wireless sensor network with  $n$  sensor nodes is deployed in the surveillance field. In the network, the total number of wireless links is  $M = n(n - 1)$ . As human presence in the surveillance field attenuates wireless links in the network, RSS readings of wireless links will change. Let  $Y_i$  denote the RSS dynamic value of the  $i$ th wireless link and  $Y = [Y_1, Y_2, \dots, Y_M]$  denote RSS dynamic values of all links. To locate a person, the surveillance field is first discretized into  $N$  voxels. Let  $X_i$  denote the attenuation introduced by a person standing at voxel  $i$  and  $X = [X_1, X_2, \dots, X_N]$  denote the attenuation of all voxels in the surveillance field. Since positions of  $N$  voxels are known beforehand, the position where the attenuation occurs in the surveillance field can be determined once  $X$  is calculated. RSS

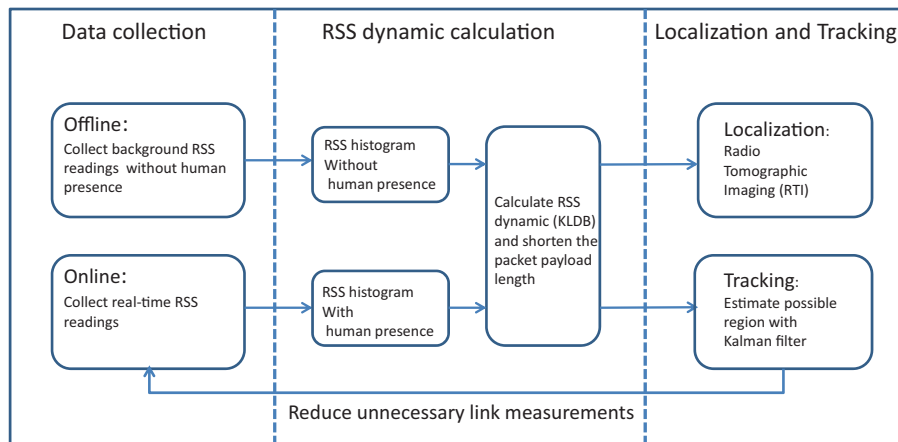


Fig. 1. EE-Loc modules.

dynamic of a wireless link is contributed by attenuation at voxels near the wireless link, and the relationship between  $X$  and  $Y$  is characterized by the following linear formulation:

$$Y = WX + noise, \quad (1)$$

where *noise* denotes the noise in the RSS readings.  $W$  represents the elliptical model that will be introduced next.

$W$  is a weight matrix of size  $M \times N$ . As the attenuation at each voxel contributes differently to RSS dynamic values of different wireless links, a weight is proposed to compensate for the difference. The attenuation matrix  $W$  is formally defined as follows:

$$W_{ij} = \frac{1}{\sqrt{d}} \begin{cases} 1, & \text{if } d_{i,j} + d_{i,j} < d + \lambda \\ 0, & \text{otherwise} \end{cases}, \quad (2)$$

where  $d_{i,j}$  is the distance between the  $j$ th voxel and the sender of the  $i$ th link and  $d_{i,j}$  is the distance between the  $j$ th voxel and the receiver of the  $i$ th link.  $d$  is the distance between the sender and receiver of the  $i$ th link.  $\lambda$  is the excess path length in the elliptical model, which is used to tune the width of the ellipse. This equation explains why the weight model is called the elliptical model. In the elliptical model, voxels in the ellipsoid with foci at two sensors of a wireless link are assumed to attenuate the link, and voxels outside the ellipsoid do not attenuate the wireless link. Given the weight matrix  $W$  and RSS dynamic vector  $Y$ , RTI is to estimate the attenuation image  $X$  and locate the person.

### 3.2. RSS histogram and KL-divergence

In this section we first describe how to get an RSS histogram from RSS readings. We then define KL-divergence to measure the difference between two RSS histograms.

For a particular link in the wireless sensor network, the receiver of the link periodically gets the RSS reading denoted as  $r_i$ . According to the TelosB datasheet [7], RSS readings from a sensor node are integers ranging from  $-90$  dBm to  $0$  dBm. Thus there is a finite set of RSS readings returned by sensors and we can construct a RSS histogram with  $91 = 0 - (-90) + 1$  bins (the bin width is  $1$  dBm) from several RSS readings in a specific time interval. For example, for a particular link in the sensor surveillance system, the receiver of the link reports a RSS reading periodically. Assume the period is  $T$ , we denote by  $r_k$  the RSS reading reported by the receiver at time  $t = kT$ . So at time  $t = nT$ , we can construct a RSS histogram  $H$  from RSS readings reported in the time window  $[(n - s + 1)T, nT]$ . Here, we denote by  $s$  the length of the time window. The  $i_{\text{th}}$  elements of  $H$  counts how many times RSS readings valued  $(-90 + i)$  dBm in the time window. When no person is present, the RSS histogram

calculated from RSS readings is denoted as the background RSS histogram. When a person appears in the ellipsoid with foci at two sensors of a wireless link, the RSS histogram calculated from RSS readings is denoted as the ‘RSS histogram with person’.

Note that the RSS histogram with person contains both the background information and the foreground information introduced by human presence. In order to get the foreground information, we need to ‘subtract’ the ‘empty-room RSS histogram’ from the ‘RSS histogram with person’. KL-divergence is often used to measure the information difference between two probability distributions in probability theory. Therefore, we adopt the KL-divergence as the RSS dynamic measure brought by human presence. The RSS dynamic value can be obtained by calculating the KL-divergence between the RSS histogram with person  $H_d$  and the background RSS histogram  $H_b$ . KL-divergence can be calculated as follows:

$$D_{KL}(H_d || H_b) = \sum_i \ln \left( \frac{\hat{H}_d(i)}{\hat{H}_b(i)} \right) \hat{H}_d(i), \quad (3)$$

where

$$\hat{H}_d(i) = \frac{\max(\epsilon, H_d(j))}{\sum_j \max(\epsilon, H_d(j))}$$

and

$$\hat{H}_b(i) = \frac{\max(\epsilon, H_b(j))}{\sum_j \max(\epsilon, H_b(j))}.$$

$\epsilon$  is a small number ( $10^{-6}$ ) that avoids divide-by-zero and  $\log 0$ .

## 4. EE-Loc overview

In this section, we present an energy efficient device free localization and tracking system called EE-Loc. EE-Loc takes RSS readings from sensors as input, and outputs the location of the person when a person appears in the surveillance field. At a high level, EE-Loc is comprised of three modules shown in Fig. 1: data collection module, RSS dynamic calculation module and localization and tracking module. The data collection module collects background RSS readings of all wireless links in the sensor network without human presence during the offline phase and collects real-time RSS readings of all links during the online phase. For each link, the RSS dynamic calculation module compares RSS readings in the two phases and produces a RSS dynamic measure. With the real-time RSS dynamics of all wireless links, the localization and tracking module locates and tracks the person in a real-time fashion.

Different from existing works on device free localization, we focus on energy efficiency in EE-Loc. There are two main energy

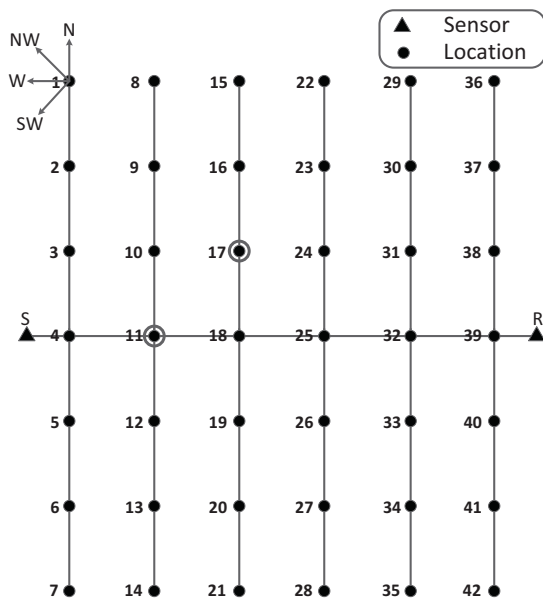


Fig. 2. The sketch for the indoor scene.

efficient mechanisms in EE-Loc. In existing works [2,6,9], RSS readings in the wireless sensor network are first transmitted to a base station, and are then processed into RSS dynamics on the PC. The RSS dynamics are later fed as input to the localization and tracking module. In EE-Loc, we design a new RSS dynamic measure (KLDB) for each wireless link with only one bit and implement the RSS dynamic calculation locally in the wireless sensor network. Compared with other DFL systems, EE-Loc reduces the payload size of each packet and implements the data collection and RSS dynamic calculation in a more energy efficient way. The second energy efficient mechanism comes from our observation that feedback from the tracking module helps reduce unnecessary links measurements in the data collection module. EE-Loc adopts Kalman filter to predict the possible region of human presence. With the person's spatial distribution calculated in the tracking module, EE-Loc can infer the person's possible region with a certain confidence level. Thus EE-Loc can deactivate many unnecessary links in the data collection module to reduce energy consumption.

## 5. EE-Loc design

We first present our empirical study of KL-divergence, and show that KL-divergence is a RSS dynamic measure compatible with the elliptical link model. Then, we derive a new RSS dynamic measure KLDB to indicate the human presence, and show how to locate a stationary person by radio tomographic imaging with one bit information. Then we define the related links of the person and show how Kalman filter can be incorporated to track a person with fewer active links. Finally we describe implementation details of EE-Loc.

### 5.1. Empirical study of KL-divergence

In this subsection, we report our empirical study on KL-divergence. We first introduce the experimental setup. Then we show that KL-divergence is compatible with the elliptical link model in our experiments and can be used as an indicator to detect whether a person is near the LOS of a link. Then we give some explanations of why KL-divergence might be a suitable RSS dynamic measure.

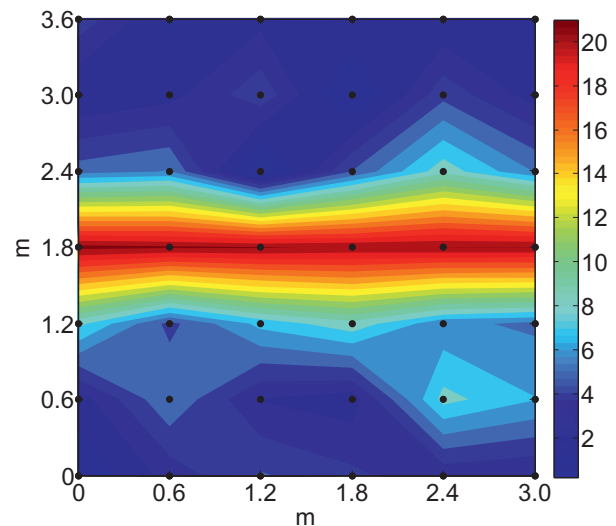


Fig. 3. The contour plot of mean KL-divergences.

In our single link experiment, we use two TelosB nodes which use the 2.4 G IEEE 802.15.4 standard for communication. We conduct the experiments in the indoor environment. The sketch for the indoor scene is shown in Fig. 2. Sensor S and sensor R are placed 3.6 m apart from each other and mounted on the tripods with height 0.9 m. 42 dots in Fig. 2 represent 42 predetermined positions where a person stands in the experiment. The distance between sensor S and position 4 is 0.3 m and the distance between position 39 and sensor R is 0.3 m. The length of all other line segments in Fig. 2 is 0.6 m. Sensor S broadcasts packets periodically and sensor R logs RSS readings of received packets. When no person is present, sensor R logs the background RSS readings. When the person stands in the predetermined positions, sensor R logs the RSS readings with person. In each predetermined positions, we collect 500 RSS readings with the person facing four directions: north, northwest, west and southwest. For each position and each orientation, KL-divergence of all wireless links in the network can be calculated with collected RSS readings. When calculating KL-divergence of the wireless link, we construct background RSS histogram from 5000 background RSS readings and construct online RSS histogram with person from the three latest RSS readings. The reason why we use only three RSS readings is as follows. We will show later in Section 6 that the sampling period is about 65.11 ms for a network with 16 sensors. This indicates the time interval during which three RSS readings are sampled is on the order of 195 ms. Considering the fact that the average human walking speed is about 1 m/s, we set  $s$  to a small value to ensure the person move a short distance away (19.5 cm) and all RSS readings sampled are useful for localization.

In our experiment, we find that KL-divergence is compatible with the elliptical link model. In the elliptical model, a person standing outside the ellipsoid with foci at two sensors of a link has little influence on the wireless link and the person standing inside the ellipsoid of the link attenuates the wireless link. Fig. 3 illustrates a contour map of mean KL-divergences of a typical wireless link with a person standing at 42 predetermined positions. Clearly, KL-divergence with person near the wireless link is larger than KL-divergence with person away from the wireless link, which is largely compatible with the elliptical model. In Fig. 4, we plot time series of KL-divergences of the wireless link when a person stands still in two representative positions (position 11 and position 17 in Fig. 2) and faces north. We can see from Fig. 2 that position 11 is on the LOS of the wireless link, while position 17 deviates from



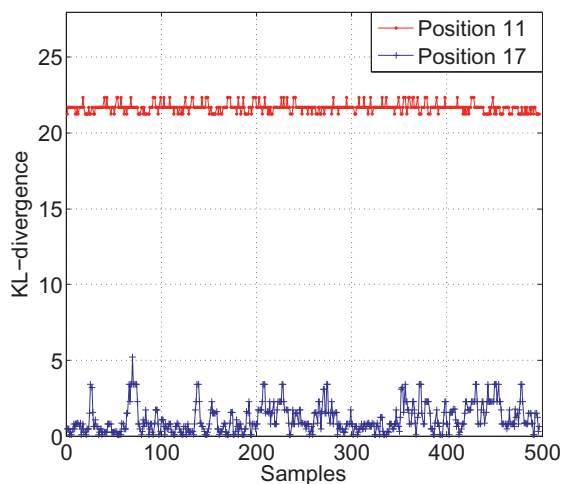


Fig. 4. Time series of KL-divergences.

LOS of the link. Fig. 4 shows that KL-divergences calculated in position 11 are always larger than KL-divergences calculated in position 17. Therefore, with a proper threshold for the link, KL-divergence can be used as a RSS dynamic measure to indicate whether the person is in the ellipsoid of the wireless link in this case.

In fact, KL-divergence can be viewed as a combination of two traditional RSS dynamic measures, mean RSS readings and variance of RSS readings. To see this, assume noise in RSS readings of a wireless link follows Gaussian distribution [4]. Under this assumption, the ‘RSS with person’ readings when a person shadows the wireless link follow a normal distribution with expectation  $\mu_1$  and variance  $\sigma_1^2$  (the distribution is denoted by  $p(x) = N(\mu_1, \sigma_1^2)$ ) and the background RSS readings when the surveillance area is vacant follow a normal distribution with expectation  $\mu_2$  and variance  $\sigma_2^2$  ( $q(x) = N(\mu_2, \sigma_2^2)$ ). According to the definition of KL-divergence, we can calculate the KL-divergence between the distribution of RSS readings with person and the distribution of background RSS readings as

$$D_{KL}(p||q) = \int [\log(p(x)) - \log(q(x))]p(x)dx$$

$$= \frac{(\mu_1 - \mu_2)^2}{2\sigma_2^2} + \frac{1}{2} \left( \frac{\sigma_1^2}{\sigma_2^2} - 1 - \log \frac{\sigma_1^2}{\sigma_2^2} \right). \quad (4)$$

As mentioned in [6], in terms of measuring the RSS dynamic caused by human presence near the wireless link, the difference of mean RSS readings performs well in LOS environment and variance of RSS readings works well in non-LOS environment. And we can see from the above equation, the KL-divergence actually incorporates both the difference between means  $(\mu_1 - \mu_2)^2$  and variance of RSS readings  $\frac{\sigma_1^2}{\sigma_2^2}$ . Thus KL-divergence is a suitable RSS dynamic measure to quantify the attenuation of a wireless link caused by human presence.

## 5.2. Radio tomographic imaging with one-bit information

In this subsection, we first introduce the KL-divergence based radio tomographic imaging. Then we present our modifications to KL-divergence based radio tomographic imaging in EE-Loc. We replace KL-divergence in radio tomographic imaging with a one-bit RSS dynamic (KLDB) derived from KL-divergence and prove that radio tomographic imaging with KLDB is sufficient to locate a person.

The relationship between the RSS dynamic value and human presence information is characterized by a linear model:  $Y = WX + \text{noise}$ , which is adopted in many RTI systems [2,6]. As mentioned in

Section 3, the voxel  $i$  of the radio tomographic image  $X_i$  contains human presence information on voxel  $i$ . When the KL-divergence is adopted as the RSS dynamic measure,  $Y_i$  represents the KL-divergence between the ‘RSS histogram with person’ and the ‘background RSS histogram’. In order to get a high resolution image, the voxel number  $N$  is sometimes set to a large value, which is larger than the number of wireless links  $M$ . This means the number of rows is less than the number of columns in  $W$ . Therefore, the radio tomographic imaging problem that computes  $X$  from an RSS dynamic vector  $Y$  is an ill-posed problem. The commonly adopted method of solving the ill-posed problem is Tikhonov regularization. In order to get  $X$ , this ill-posed problem is replaced by an equivalent optimization problem

$$\operatorname{argmin}_X ||WX - Y||^2 + \delta ||X||^2, \quad (5)$$

where  $\delta$  is a parameter that controls the tradeoff between norm of error  $WX - Y$  and norm of  $X$ . The solution of the optimization problem is:  $X = VD_\delta^+ U^T Y$ , where  $D_\delta^+ = \operatorname{diag}(\frac{d_1}{d_1^2 + \delta}, \dots, \frac{d_{\min(M,N)}}{d_{\min(M,N)}^2 + \delta})$ , where  $U$  and  $V$  are derived from singular value decomposition of  $W$  ( $W = UDV^T$ ) and  $d_i$  is  $i$ th the diagonal element of  $D$ . Note that in practice  $VD_\delta^+ U^T$  can be calculated offline once and stored on a PC for later computations. After the KL-divergence vector  $Y$  is calculated on a PC from RSS readings reported by sensors,  $X$  can be calculated online with time complexity  $O(MN)$ . The magnitude of the  $i$ th element  $X_i$  in  $X$  represents the likelihood of human presence on the  $i$ th voxel. With the mapping between voxel’s index and the voxel’s location  $L_i$ , the person’s location can be inferred with a weighted average method. For ease of description, assume  $X$  is already sorted in descending order, the location of the person can be estimated by the weighted average of the first  $T$  elements’ location

$$L_{\text{person}} = \sum_{i=1}^T |X'_i| L_i.$$

Instead of KL-divergence vector  $Y$ , we use a bit vector  $Y'$  composed of binarized KL-divergence (KLDBs) in EE-Loc. The  $j$ th element of  $Y'$ , denoted by  $Y'_j$ , is derived from KL-divergence of link  $j$  with ‘thresholding’.  $Y'_j$  is equal to 0 when  $Y_j \leq \text{threshold}$ , otherwise  $Y'_j$  is equal to 1. The parameter *threshold* can be determined by experimental data. Take the data in Fig. 4 for example. Position 11 represents the KL-divergence near LOS with mean 21.66 and position 17 represents the KL-divergence away from LOS with mean 1.11. The *threshold* is set to  $\frac{21.66 + 1.11}{2} = 11.385$ .  $Y'_j$  indicates whether a person is in the ellipsoid of wireless link  $i$ . We show in the following theorem that if wireless links report correct KLDB values, radio tomographic imaging with one-bit KLDB is sufficient to locate the person.

**Theorem 1.** Suppose matrix  $W$  is defined according to Eq. (2), and  $X \in [0, 1]^N$  is a vector indicating the likelihood of human presence in the surveillance field, where  $N$  denotes the total number of voxels. Assume a person can stand at a voxel at a time. Let  $Y' \in \{0, 1\}^M$  denote binarized KL-divergence vector such that  $Y'_j = 1$  if and only if the person stands at voxel  $i$  in the ellipsoid of wireless link  $j$ , where  $M$  is the number of wireless links. Let  $d_{\min}$  denote the shortest link length. Then, after solving the optimization problem  $\operatorname{argmin}_{X \in [0,1]^N} ||WX - Y'||^2 + \delta ||X||^2$  where  $\delta \geq \frac{M \cdot N^2}{d_{\min}^2}$ , the voxel  $i$  where the person stands has the highest  $X_i$  value.

**Proof.** Suppose voxel  $i$  is in the ellipsoid of wireless links  $l_1, l_2, \dots, l_s$ . Let voxel  $j$  be away from the person’s location and in the ellipsoid of wireless links  $l'_1, l'_2, \dots, l'_t$ . As voxel  $i$  is the voxel where the person stands, the items which contain  $X_i$  in the objective function  $||WX - Y'||^2 + \delta ||X||^2$  can be written as

$(\frac{1}{\sqrt{d_{l_1}}}X_i + \frac{1}{\sqrt{d_{l_1}}}X_j + \dots - 1)^2 + \dots + (\frac{1}{\sqrt{d_{l_s}}}X_i + \frac{1}{\sqrt{d_{l_s}}}X_k + \dots - 1)^2 + \delta X_i^2$ . As voxel  $j$  is away from the position where the person stands, the items which contain  $X_j$  in the objective function can be written as  $(\frac{1}{\sqrt{d_{l'_1}}}X_i + \frac{1}{\sqrt{d_{l'_1}}}X_j + \dots - 1)^2 + \dots + (\frac{1}{\sqrt{d_{l'_t}}}X_j + \frac{1}{\sqrt{d_{l'_t}}}X_p + \dots - 0)^2 + \delta X_j^2$ . Suppose that  $X_j$  is larger than  $X_i$  in the optimal solution  $X$ , then we can construct a new solution  $X'$  from  $X$  by swapping  $X_i$  and  $X_j$ . In the following, we show that the objective value of  $X'$  is smaller than that of  $X$ , which leads to a contradiction.

Notice that links covering voxel  $j$  with KLDB 1 is a subset of links covering voxel  $i$ . For links covering both voxel  $i$  and voxel  $j$ , swapping the two elements will not change the value of  $(\frac{1}{\sqrt{d_{l_1}}}X_i + \frac{1}{\sqrt{d_{l_1}}}X_j + \dots - 1)^2$ . Similarly, the value of  $\delta X_i^2 + \delta X_j^2$  will not change after swapping  $X_i$  and  $X_j$ . For links covering voxel  $j$  only, take the link covering voxel  $j$  and voxel  $p$  as an example, swapping the two elements decreases the value of  $(\frac{1}{\sqrt{d_{l'_t}}}X_j + \frac{1}{\sqrt{d_{l'_t}}}X_p + \dots - 0)^2$ .

For links covering voxel  $i$  only, take the link covering voxel  $i$  and voxel  $k$  as an example, if we can prove that the value of  $(\frac{1}{\sqrt{d_{l_s}}}X_i + \frac{1}{\sqrt{d_{l_s}}}X_k + \dots - 1)^2$  decreases after we swap  $X_i$  and  $X_j$ , then we derive a contradiction that  $X$  is not optimal. When  $\delta \geq \frac{M \cdot N^2}{d_{min}^2}$ , elements in  $X$  are less than  $\frac{d_{min}}{N}$  and increasing  $X_i$  will decrease the value of  $(\frac{1}{\sqrt{d_{l_s}}}X_i + \frac{1}{\sqrt{d_{l_s}}}X_k + \dots - 1)^2$ . However, this contradicts the original assumption that  $X$  is optimal, which completes the proof.  $\square$

Using the new RSS dynamic measure KLDB can save energy due to reduced packet payload size. The underlying reason why we can use binary KLDB values in the RTI is that we do not need the exact  $X_i$  value in Eq. (5) to locate the person in the surveillance field. Only the ranking of  $X_i$  matters. To this end, binary KLDB values of wireless links provide sufficient information to distinguish the ranking of  $X_i$ .

### 5.3. Tracking with fewer active links

Different from directly using Kalman filter to smooth the trace of the person, we utilize Kalman filter to improve energy efficiency of the DFL system. When the person is moving in the surveillance area, the next possible region of human presence can be predicted beforehand by Kalman filter. With the predicted region of human presence, only links related to the next possible region of the person are involved in logging the RSS measurements and RSS measurements of other links are not necessary. In this way, we can achieve tracking with fewer active links.

In our online DFL system, sensors in the surveillance system send packets one after another in a round-robin mode. When one sensor is broadcasting a packet, all other sensors in the system log the RSS measurements and calculate the KL-divergences of wireless links. After all sensors reports the RSS dynamic values to the base station at time  $t$ , the KL-divergence based RTI can be utilized to locate the person. Thus, by time  $t$  we have a time series of person's locations  $L_i = \langle x_i, y_i \rangle, i = 1 \dots t$ . Assuming that the unknown location of human presence follows a linear Gaussian distribution, we can apply Kalman filter to the time series of the person's location. The temporal model used with Kalman filter is formally listed as follows:

$$P(L_{t+1}|L_t) = N(FL_t, \Sigma_L)(L_{t+1}) \tag{6}$$

$$P(L'_t|L_t) = N(HL_t, \Sigma_{L'}) (L'_t),$$

where  $F$  and  $\Sigma_L$  describe the linear transition model and noise covariance in the transition model and  $H$  and  $\Sigma_{L'}$  describe the

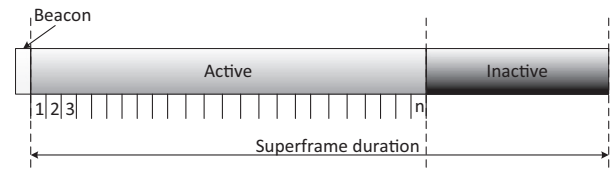


Fig. 5. Superframe structure.

measurement model and noise covariance in the measurement model. With Eq. (6), the possible region of human presence at time  $t + 1$  can be predicted at time  $t$ . With the possible region of human presence predicted by Kalman filter, RSS measurements of wireless links unrelated to the possible region can be omitted. Here we call a wireless link is unrelated when voxels in the possible region of human presence do not intersect the ellipsoid of the wireless link. As unrelated links offer no benefits to locate the person, RSS measurements of the unrelated links can be safely eliminated. In our DFL system, prior to a round of RSS measurements, the base station first broadcasts a packet indicating which links are involved in the following round of RSS measurements. Receivers of the unrelated links are able to turn off their radios to save energy in the next round. In this way, the base station may receive meaningless RSS dynamic values of unrelated links as the receivers do not make the RSS measurements. This issue can be easily fixed by the following trick. After collecting the RSS dynamic values of all sensors, KLDBs of the unrelated links in the RSS dynamic vector  $Y'$  are set to 0 since the base station knows which links are involved in the round.

We need to mention that there is a trade-off between localization accuracy and energy efficiency. In the extreme case that the person changes speed and direction abruptly, it is difficult to predict the next possible region and we need to activate all wireless links. Fortunately, in most cases, it is possible to predict the next possible region of a person, so we can safely reduce unnecessary link measurements to save energy.

### 5.4. Protocol and implementation

In this subsection, we first describe the superframe structure and the flow chart of our protocol. Then implementation details of EE-Loc are given.

Fig. 5 illustrates the format of the superframe structure. There are three parts in superframe, namely a beacon part, an active part and an inactive part. In the beacon part, sensors in the network receive packets from the base station, which indicate the related links. The active part is further divided into  $n$  slots ( $n$  is the number of sensors). Assume we assign IDs  $1 \dots n$  to sensors, Sensor  $i$  is scheduled to send a broadcast packet containing KLDBs of links in Slot  $i$ . In Slot  $i$ , other sensors log the RSS readings of the broadcast packet and calculate KLDB of corresponding links from RSS readings. In the meantime, the base station can overhear the broadcast packet and collect the KLDB values contained in the broadcast packet. In the inactive part all sensors are scheduled to enter the low power mode. Repeating the superframe structure, we actually operate sensors in a duty-cycling work mode. If the duration of the inactive part is 0, the sensor network is always in the active part. Therefore, sensors in the system take turns to send a broadcast packet one by one. Fig. 6 illustrates the flow chart of the protocol, which shows the interaction between the base station and sensors in the sensor network. When tracking a moving person, the base station can predict the possible region of the person in the next time step and broadcasts the related links to sensors in the network. During the active part of the superframe, the receiver of the

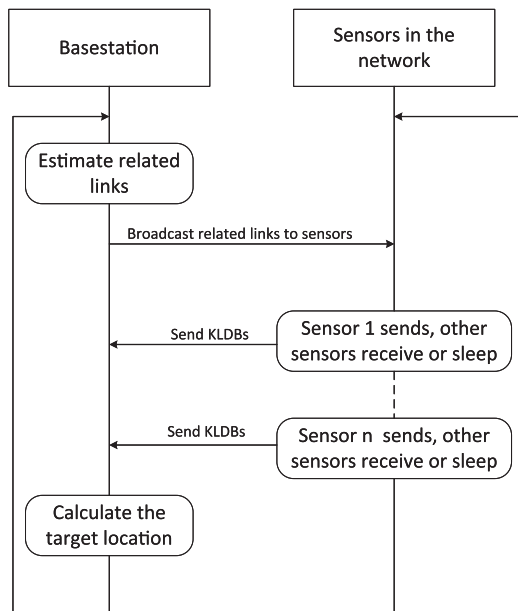


Fig. 6. Interaction between the base station and sensors.



Fig. 7. Indoor test field.

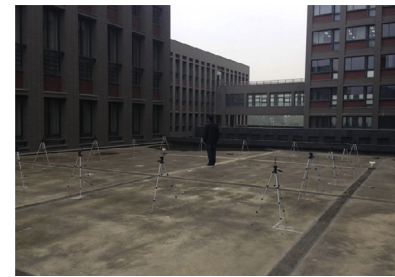


Fig. 8. Outdoor test field.

link can choose to receive the broadcast packet or to enter the low power mode depending on whether it is receiver of a related link.

We implement EE-Loc based on Spin [2]. We make three modifications to the Spin protocol. The first modification is that we change the data type of  $RSS[NUM\_NODES]$  into  $nx\_int8\_t$ .  $nx\_int16\_t$  used in the original Spin will increase the payload of the packet and is not necessary since the return type of  $CC2420Packet.getRssi$  is  $nx\_int8\_t$ . Since TDMA is adopted in our protocol, the random backoff before CCA (clear channel assessment) is unnecessary. Therefore, the second modification is that we use the interface *RadioBackoff* of *CC2420ActiveMessageC* to eliminate the initial backoff before CCA. The third modification is that sensors calculate the RSS dynamic vector locally and transmit KLDBs instead of raw RSS readings. As we know, calculating  $\log$  function in the TelosB platform is time consuming. One concern of KLDB is the high computation cost of KL-divergence. For simplicity, we calculate the  $\log$  values beforehand and store them in a table for future table lookup.

## 6. Experiments

We first present our experimental setup. We then evaluate the energy efficiency of EE-Loc in terms of sweep latency. Despite of the fact that EE-Loc transmits less bits and uses less links, our experimental results show that the performance of EE-Loc is comparable to the accuracy of the state-of-the-art DFL systems.

### 6.1. Experimental setup

The sensor nodes used in our experiments are TelosB sensor nodes with 2.4 GHz IEEE 802.15.4 compliant CC2420 radio transceivers. IEEE 802.15.4 specifies 16 channels within the 2.4 GHz band, numbered 11–26. We use the 26th channel (central frequency is 2.48 GHz) for wireless transmission. We conduct our experiments in both indoor and outdoor environments. The indoor experiment comprises a wireless sensor network with 16 TelosB sensors deployed on adjustable tripods with height 0.9 m along the perimeter of  $3.6\text{ m} \times 3.6\text{ m}$  square. The distance between adjacent sensors is 0.9 m. The 16 sensors broadcast a packet one after another with default transmission power 0 dBm. A base station overhears all wireless transmissions, and then feeds the packets to

a computer via a USB port. The computer then runs the localization and tracking algorithms to locate and track the person. The photo of the experiment setup is shown in Fig. 7. Similarly, in the outdoor experiment, we deploy a wireless sensor network on 16 adjustable tripods with height 0.9 m along the perimeter of  $8\text{ m} \times 8\text{ m}$  square. The distance between adjacent sensors is 2 m. The photograph of the experimental scene is shown in Fig. 8.

### 6.2. Sweep latency

The sweep latency depends on how much time for sensors in a DFL system to sweep the surveillance area once. Indeed, the sweep latency is the duration of the active part in the superframe. Consequently, if we shorten the sweep latency, we can reduce the duration of active part. In other words, shorter sweep latency leads to a lower duty cycle for DFL systems. In the following, we compare KLDB with Spin\*, an enhanced version of Spin [2], in terms of the sweep latency. The sweep latency is directly related to the payload size of packets. In our experiments, we have 16 sensors in the wireless sensor network. If we use the Spin\* protocol to collect data, the packet payload length is 17 bytes ( $nx\_int8\_t\ nodeid$  and  $nx\_int8\_t\ RSSI[NUM\_NODES]$ ). But in EE-Loc, we can reduce the payload length from 17 bytes to 3 bytes ( $nx\_int8\_t\ nodeid$  and  $nx\_uint16\_t\ KLDB$ ). Here,  $nodeid$  is the id of the receiver. The  $i$ th element of  $RSSI[NUM\_NODES]$  is received signal strength measured at the receiver when sensor  $i$  broadcasts a packet. The  $i$ th bit of KLDB is an indicator indicating whether the wireless link between sensor  $i$  and the receiver is attenuated or not. Generally, when the number of nodes is  $n$ , EE-Loc can reduce the payload size from  $n + 1$  bytes to  $\lceil \frac{n}{8} \rceil + 1$  bytes. As the payload size is greatly shortened, we expect the latency of collecting KLDBs in EE-Loc is shorter than collecting raw RSS readings in Spin\*.

Spin collects RSS readings using a token passing protocol. For a fair comparison, we make the first two modifications to the Spin as we do in EE-Loc. We refer to the modified Spin as Spin\*. To assess the overhead of calculating KLDBs, we comment out the part of computing KL-divergences in the KLDB code. We denote the KLDB without calculating KL-divergence as KLDB\*. We implement the three protocols in the testbed and run the protocols

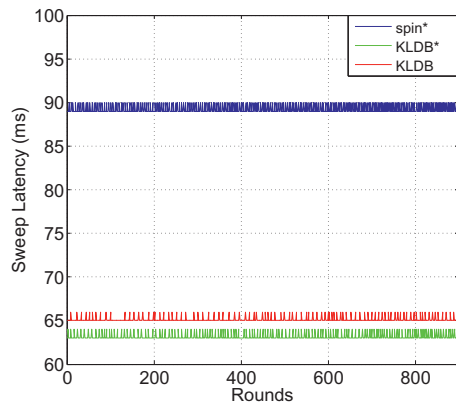


Fig. 9. The sweep latency.

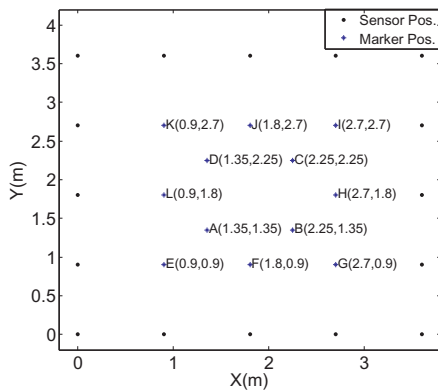


Fig. 10. Position of sensors and markers.

1000 rounds respectively. We show the sweep latency of the three protocols in Fig. 9. Mean of sweep latency of Spin\* is 89.25 ms and mean of sweep latency of KLDB is 65.11 ms. KLDB shortens the sweep latency of Spin\* by 27.05%. In Fig. 9, we can see that the sweep latency of KLDB\* is slightly lower than KLDB, which shows the computation of KL-divergences is efficiently implemented with the table lookup.

If Spin\* is used in a DFL system and the length of the inactive part of a superframe is 0, shortening the sweep latency of Spin\* with KLDB means lowering the duty cycle of wireless sensor network by 27.05% without harming the sample rate of RSS in the DFL system. As KLDB is adopted, the inactive part of a superframe increases. Thus compared with Spin\*, KLDB improves the energy efficiency by 27.05% in each round.

### 6.3. Localization accuracy in indoor environments

To evaluate the localization performance, we mark 12 locations in the surveillance area. We have a person stand still with 8 different orientations in the 12 locations and log the RSS measurements of all links in the PC. The 12 locations are showed in Fig. 10. For comparison, we implement three additional algorithms: link difference based RTI (IdRTI) [2], KLD [6], CMMS [19]. All four algorithms share a common model: they adopt the same linear model characterizing the relationship between the RSS dynamic vector and attenuation on the voxels. The difference lies in how to solve the linear equation and the choice of the RSS dynamic measure. In IdRTI, KLD and our algorithm (KLDB for short), Tikhonov regularization is utilized to solve the linear equation. While in CMMS, the unknown attenuation positions are deemed as the sparse signals and a lightweight compressive sensing based RTI is utilized to recover the sparse signal. As for

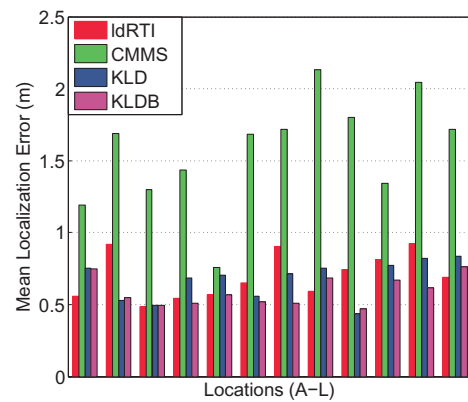


Fig. 11. Mean localization error.

Table 1

Parameters used in the evaluation.

Parameter	Value
$\lambda$ in the elliptical model	0.03
$\epsilon$ in KL-divergence	$1e-6$
side length of a voxel	0.15
$\delta$ in the Tikhonov regularization	5
$T$ in the localization algorithm	10

the choice of the RSS dynamic measure, the RSS dynamic measure in our algorithm is KLDB. In IdRTI and CMMS, the RSS dynamic value of a link is characterized by difference between mean RSS readings in a short time window and mean RSS readings in a calibration step when the surveillance area is vacant. With the logged RSS measurements of all links, we use the 4 algorithms to locate the person. As we know the exact position of 12 locations, the metric used in the evaluation is mean localization error, which is defined as the Euclidean distance between the ground truth and the estimated position. In Fig. 11, we plot the mean localization error of 4 algorithms in 12 test positions (A–L). Some important parameters used in the algorithms are listed in Table 1.  $T$  is equal to 1 in CMMS and *Threshold* in KLDB is set to 17. We can see from Fig. 11 that KLD and KLDB outperform IdRTI and CMMS in most test positions. The performance of KLDB is roughly the same as that of KLD. Note that in KLDB, sensors are required to send 1-bit indicator variable instead of the raw 8-bit RSS reading of each wireless link to the base station. Taking the payload length of the transmitting packets into consideration, KLDB is much better than KLD.

### 6.4. Tracking performance in outdoor environments

To verify the tracking performance of KLDB and the Kalman filter based related links scheme, we have a person walk around a square at a constant speed in the surveillance area. During the experiment we collect 296 RSS dynamic vectors. Since we know the walking path of the person, the actual position of the person (ground truth) when the RSS vector is collected can be obtained by interpolation. With the RSS dynamic vectors, we can infer the location of the person when the RSS dynamic vector is sampled. The localization error is defined as the deviation between the estimated position and the ground truth. Mean localization error is defined as the mean of 296 localization errors. In Fig. 12, we show the results of two estimated paths (use KL-divergence and KLDB as the RSS dynamic measure separately) of the person with EE-Loc. We can see that the estimated trace generally agrees with the ground truth. The mean localization error of KLD is 0.66 m and STD of estimated errors of 296 predictions is 0.41 m. The mean



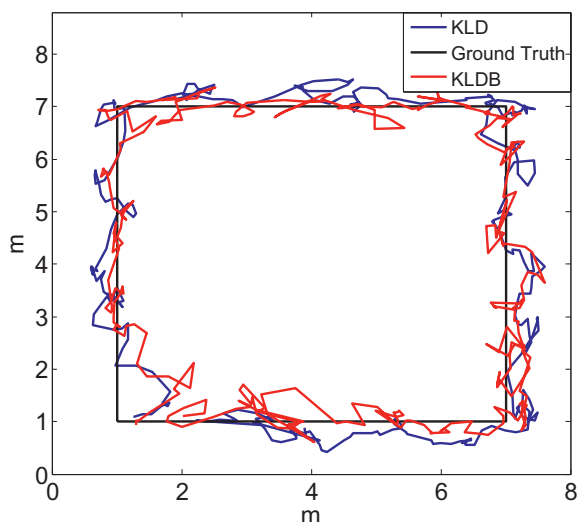


Fig. 12. Estimated trace.

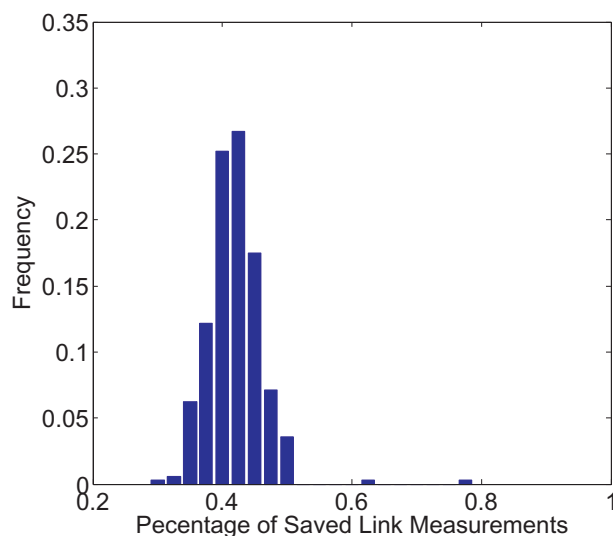


Fig. 13. Percentage of deactivated links.

localization error of KLDB, which outperforms KLD, is 0.54 m and STD of estimated errors is 0.32 m. As EE-Loc can predict the related links before the actual link measurements, some link measurements can be saved in the next round of RSS measurements. The receivers not involved in the link measurements can turn off their radio module to save energy. Fig. 13 shows the histogram of percentage of saved measurements in 296 rounds of RSS measurements. The x-axis of Fig. 13 denotes the percentage of link measurements which can be saved in a round of RSS measurements. The mean of the saved link measurements percentage is 41.91% with EE-Loc.

## 7. Conclusions

In this paper, we propose EE-Loc to locate and track a person in the surveillance area. By reducing the payload of packets with a new RSS dynamic measure KLDB and deactivating unrelated links with Kalman filter, we improve the energy efficiency of DFL sys-

tems. Two experiments are conducted in both indoor and outdoor environments. The indoor experiment shows that the localization accuracy of EE-Loc is comparable to the state-of-the-art while reducing the length of packet payload. With the payload reduction, EE-Loc improves the energy efficiency of DFL systems by 27.05% compared with Spin\*. In the outdoor experiment, EE-Loc further reduces the necessary link measurements in a round by 41.91%. In our future work, we will consider multiple target tracking with EE-Loc, as well as investigate our system for localization and tracking in more challenging indoor and outdoor scenarios, where foreign obstacles are included inside the surveillance field.

## Acknowledgments

The authors would like to thank Wei Wang for valuable discussions and Baoqian Shi for helping us with our experiments. This work is partly supported by National Natural Science Foundation of China (61133006, 61321491, 61502232 and 61373130), China Postdoctoral Science Foundation (2015M570445) and China 973 projects (2014CB340300, 2012CB316200).

## References

- [1] M. Seifeldin, M. Youssef, A deterministic large-scale device-free passive localization system for wireless environments, in: Proceedings of the PETRA, 2010.
- [2] J. Wilson, N. Patwari, Radio tomographic imaging with wireless networks, *IEEE Trans. Mob. Comput.* 9 (5) (2010) 621–632.
- [3] D. Zhang, J. Ma, Q. Chen, L.M. Ni, An RF-based system for tracking transceiver-free objects, in: Proceedings of the PerCom, 2007, pp. 135–144.
- [4] X. Chen, A. Edelstein, Y. Li, M. Coates, M.G. Rabbat, A. Men, Sequential Monte Carlo for simultaneous passive device-free tracking and sensor localization using received signal strength measurements, in: Proceedings of the IPSN, 2011, pp. 342–353.
- [5] C. Xu, B. Firner, R.S. Moore, Y. Zhang, W. Trappe, R. Howard, F. Zhang, N. An, SCPL: indoor device-free multi-subject counting and localization using radio signal strength, in: Proceedings of the IPSN, 2013, pp. 79–90.
- [6] Y. Zhao, N. Patwari, J.M. Phillips, S. Venkatasubramanian, Radio tomographic imaging and tracking of stationary and moving people via kernel distance, in: Proceedings of the IPSN, 2013, pp. 229–240.
- [7] Telosb datasheet, [www.willow.co.uk/TelosB\\_Datasheet.pdf](http://www.willow.co.uk/TelosB_Datasheet.pdf). (accessed 01.05.14)
- [8] M. Youssef, M. Mah, A.K. Agrawala, Challenges: device-free passive localization for wireless environments, in: Proceedings of the MOBICOM, 2007, pp. 222–229.
- [9] J. Wilson, N. Patwari, See-through walls: motion tracking using variance-based radio tomography networks, *IEEE Trans. Mob. Comput.* 10 (5) (2011) 612–621.
- [10] X. Zhu, X. Wu, G. Chen, Relative localization for wireless sensor networks with linear topology, *Comput. Commun.* 36 (15–16) (2013) 1581–1591.
- [11] X. Zhu, Q. Li, G. Chen, APT: accurate outdoor pedestrian tracking with smartphones, in: Proceedings of the INFOCOM, 2013, pp. 2508–2516.
- [12] D. Zhang, Y. Liu, X. Guo, L.M. Ni, Rass: A real-time, accurate, and scalable system for tracking transceiver-free objects, *IEEE Trans. Parallel Distrib. Syst.* 24 (5) (2013) 996–1008.
- [13] M. Seifeldin, A. El-keyi, M. Youssef, Kalman filter-based tracking of a device-free passive entity in wireless environments, in: Proceedings of the WiNTECH, 2011.
- [14] D. Zhang, Y. Liu, L.M. Ni, Link-centric probabilistic coverage model for transceiver-free object detection in wireless networks, in: Proceedings of the ICDCS, 2010, pp. 116–125.
- [15] J. Wilson, N. Patwari, A fade-level skew-laplace signal strength model for device-free localization with wireless networks, *IEEE Trans. Mob. Comput.* 11 (6) (2012) 947–958.
- [16] Y. Zhao, N. Patwari, Noise reduction for variance-based device-free localization and tracking, in: Proceedings of the SECON, 2011, pp. 179–187.
- [17] Y. Zheng, A. Men, Through-wall tracking with radio tomography networks using foreground detection, in: Proceedings of the WCNC, 2012, pp. 3278–3283.
- [18] C. Xu, B. Firner, Y. Zhang, R. Howard, J. Li, X. Lin, Improving RF-based device-free passive localization in cluttered indoor environments through probabilistic classification methods, in: Proceedings of the IPSN, 2012, pp. 209–220.
- [19] Z. Yang, K. Huang, X. Guo, G. Wang, A real-time device-free localization system using correlated RSS measurements, *EURASIP J. Wirel. Commun. Netw.* 2013 (2013) 186.
- [20] J. Wang, D. Fang, X. Chen, Z. Yang, T. Xing, L. Cai, Lcs: Compressive sensing based device-free localization for multiple targets in sensor networks, in: Proceedings of the INFOCOM, 2013, pp. 145–149.